Ultraslow fluctuations in the pseudogap states of $HgBa_2CaCu_2O_{6+\delta}$

Yutaka Itoh,[1,*] Takato Machi,[2] and Ayako Yamamoto[3]

[1]*Department of Physics, Graduate School of Science, Kyoto Sangyo University, Kamigamo-Motoyama, Kika-ku, Kyoto 603-8555, Japan*

[2]*AIST Tsukuba East, Research Institute for Energy Conservation, 1-2-1 Namiki, Tsukuba, Ibaraki 305-8564, Japan*

[3]*Graduate School of Engineering and Science, Shibaura Institute of Technology, 3-7-5 Toyosu, Koto-ku, Tokyo 135-8548, Japan*

(Received 29 November 2016; revised manuscript received 10 January 2017; published 6 March 2017)

We report the transverse relaxation rates $1/T_2$'s of the ^{63}Cu nuclear spin-echo envelope for double-layer high-T_c cuprate superconductors $HgBa_2CaCu_2O_{6+\delta}$ from underdoped to overdoped. The relaxation rate $1/T_{2L}$ of the exponential function (Lorentzian component) shows a peak at 220–240 K in the underdoped ($T_c = 103$ K) and the optimally doped ($T_c = 127$ K) samples but no peak in the overdoped ($T_c = 93$ K) sample. The enhancement in $1/T_{2L}$ suggests a development of the zero frequency components of local field fluctuations. Ultraslow fluctuations are hidden in the pseudogap states.

DOI: 10.1103/PhysRevB.95.094501

I. INTRODUCTION

Normal state precursory diamagnetism [1–3], a magnetic-field-induced charge-stripe order [4], and a short-range charge density wave order [5,6] have renewed our interests in the pseudogap states of high-T_c cuprate superconductors. The nature of the pseudogap state has been one of the central issues in studying strong correlation effects.

We focus on the transverse relaxation of nuclear spins in the system. For the typical high-T_c cuprate superconductor $YBa_2Cu_3O_7$ in a static magnetic field along the c axis, the plane-site Cu nuclear spin-echo transverse relaxation is caused by indirect nuclear spin-spin coupling via electron spin fluctuations and the nuclear spin-lattice relaxation process due to electron spin fluctuations [7,8]. Static nuclear spin-spin coupling leads to a Gaussian relaxation function with a time constant T_{2G}, that is, a spin-echo amplitude $E(t)$ at time t as $E(t) \propto \exp[-\frac{1}{2}(t/T_{2G})^2]$ [7,8]. Electron spin fluctuations lead to a single exponential relaxation function with a time constant T_2 (T_1 process) associated with a nuclear spin-lattice relaxation time T_1 using the Redfield theory, that is, $E(t) \propto \exp(-t/T_2)$ [7,9]. The Cu nuclear spin-echo transverse relaxation curve is expressed by the product of the exponential and Gaussian functions in the static limit of $T_1 \gg T_{2G}$, that is, $E(t) = E(0)\exp[-t/T_2 - \frac{1}{2}(t/T_{2G})^2]$.

The nuclear spin-lattice relaxation rate divided by temperature $1/T_1T$ is associated with the low frequency part of the dynamical spin susceptibility $\chi''(\boldsymbol{q},\omega)$ (q is a wave vector, and ω is a frequency) of unpaired electrons [10], while the Gaussian relaxation rate $1/T_{2G}$ is associated with the static staggered spin susceptibility $\chi'(\boldsymbol{Q})$ (Q is the antiferromagnetic wave vector) [8,11]. $\chi'(\boldsymbol{Q})$ is related to $\chi''(\boldsymbol{Q},\omega)$ through the Kramers-Kronig relation. The temperature dependence of $\chi'(\boldsymbol{Q})$ through $1/T_{2G}$ for the high-T_c cuprate superconductors tells us the $d_{x^2-y^2}$ wave pairing symmetry in the superconducting state [12], the self-consistently renormalized spin fluctuation effects on the Curie-Weiss-type antiferromagnetic correlation length [13], and the spin-pseudogap spectrum [12,14]. Dynamic scaling laws on $\chi''(\boldsymbol{q},\omega)$ for low-dimensional antiferromagnetic Heisenberg systems have been tested by measurements of $1/T_{2G}$ [15,16]. Thus, the Gaussian decay rate $1/T_{2G}$ has provided us with rich information on the microscopic properties of the correlated materials. In this paper, however, our main concern is a transverse relaxation time T_2 due to the T_1 process (Lorentzian component) but not the Gaussian decay time T_{2G}.

To be exact, a longitudinal nuclear (spin-lattice) relaxation time T_1 and a transverse relaxation time T_2 (T_1 process) are caused by different frequency parts of the local field fluctuations [10]. For convenience, let us assume a nuclear spin $I = \frac{1}{2}$. T_1 probes the transverse fluctuation $J_\perp(\nu_n)$ at a Larmor frequency ν_n as $1/T_1 = 2J_\perp(\nu_n)$, while T_2 probes the additional longitudinal fluctuation at the zero frequency as $1/T_2 = 1/2T_1 + J_\parallel(0)$ [9,10,17]. Zero frequency fluctuations represent ultraslow dynamics of the system, e.g., glassy nature and frustration effects. Glassy charge-spin stripe orderings with ultraslow fluctuations and wipeout effects have been observed by nuclear quadrupole resonance (NQR) measurements for the La-based 214 family [18–20].

If the longitudinal fluctuation at zero frequency is equal to that at the Larmor frequency as $J_\parallel(0) = J_\parallel(\nu_n)$, T_2 can be estimated from T_1 using the Redfield theory [9]. The T_2 estimated from the experimental T_1 is denoted as T_{2R}, after Ref. [7]. The experimental T_2 in the exponential time development of the transverse relaxation function is denoted as T_{2L}.

$HgBa_2CaCu_2O_{6+\delta}$ (Hg1212) is a double-CuO_2-layer system of the high-T_c cuprate superconductors [21]. The optimized T_c of about 127 K is the highest among the reported double-layer cuprate superconductors, which is associated with the flatness of the CuO_2 planes in a unit cell [21,22]. Not only high T_c but also large-scale pseudogaps turned out to characterize Hg1212 even at the optimally doping level through Cu NMR studies [14].

In this paper, we report the ^{63}Cu nuclear spin-echo transverse relaxation rates for Hg1212 with $T_c = 103$ K at the underdoping level, 127 K at the optimally doping level, and 93 K at the overdoping level. We found a strong enhancement in the transverse relaxation rate $1/T_{2L}$ of the exponential function at 220–240 K for the underdoped and optimally doped samples, which could not be explained by anisotropic ^{63}Cu nuclear spin-lattice relaxation times. The peak in $1/T_{2L}$ at

*yitoh@cc.kyoto-su.ac.jp

 ©2017 American Physical Society

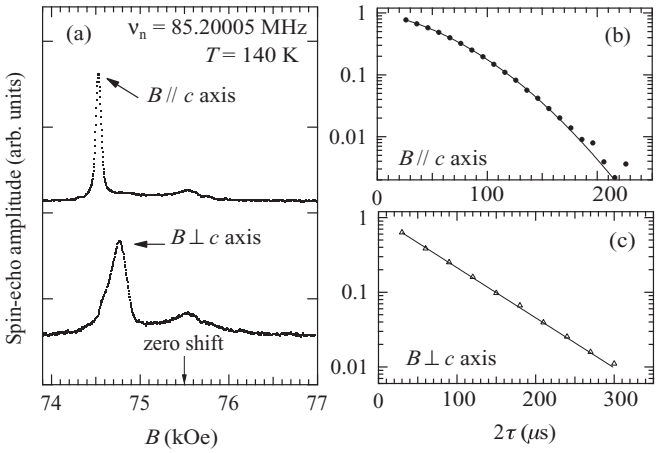

FIG. 1. (a) Central transition lines ($I_z = \frac{1}{2} \leftrightarrow -\frac{1}{2}$) of field-swept quadrupole-split ^{63}Cu NMR spectra ($B \parallel c$ axis and $B \perp c$ axis) for the optimally doped Hg1212 ($T_c = 127$ K) at 140 K and 85.2 MHz. Transverse relaxation curves $E(2\tau)$ of the ^{63}Cu nuclear spin echoes for (b) $B \parallel c$ axis and (c) $B \perp c$ axis.

220–240 K suggests the emergence of different zero frequency fluctuations in the pseudogap states.

II. EXPERIMENTS

NMR experiments were performed for magnetically c axis aligned powder samples of Hg1212. The samples were prepared and characterized in Ref. [22]. A phase-coherent-type pulsed spectrometer was utilized to perform the ^{63}Cu NMR (nuclear spin $I = \frac{3}{2}$) experiments at 85.2 MHz (∼7.45 T). Most of the ^{63}Cu NMR results have already been published in Ref. [14], except for the present T_2 data. The time development of the ^{63}Cu nuclear spin-echo envelope was measured by recording the spin-echo amplitude $E(2\tau)$ following a sequence of $\pi/2$-τ-π pulses.

The ^{63}Cu nuclear spin-echo transverse relaxation curves $E(2\tau)$ were analyzed by

$$E(2\tau) = E(0)\exp\left[-\frac{2\tau}{T_{2L}} - \frac{1}{2}\left(\frac{2\tau}{T_{2G}}\right)^2\right] f(2\tau), \qquad (1)$$

where $E(0)$, T_{2L}, and T_{2G} are the fitting parameters [7]. $f(2\tau)$ is the correction function of the I_z fluctuation effects and $\ln f(2\tau)$ consists of the higher-order terms of τ^3 and τ^4 given in Refs. [23,24]. The Gaussian decay rate $1/T_{2G}$ is a measure of the indirect nuclear spin-spin coupling constant [7,8,11]. The present Gaussian decay rates $1/T_{2G}$'s were estimated by including the correction of the I_z fluctuation effect. The uncorrected $1/T_{2G}$'s, being overestimated, have been reported in Ref. [14]. We also report $1/T_{2L}$.

Figure 1(a) shows the central transition lines ($I_z = \frac{1}{2} \leftrightarrow -\frac{1}{2}$) of the field-swept quadrupole-split ^{63}Cu NMR spectra in an external magnetic field B along the oriented c axis ($B \parallel c$) and perpendicular to the c axis ($B \perp c$) for the optimally doped Hg1212 ($T_c = 127$ K) at 140 K and 85.2 MHz. The full width at half maximum of the central transition line is about 76 G for the $B \parallel c$ axis and about 230 G for the $B \perp c$ axis. The $\pi/2$ pulse of $H_1 \sim 100$ G can excite all the relevant nuclear spins

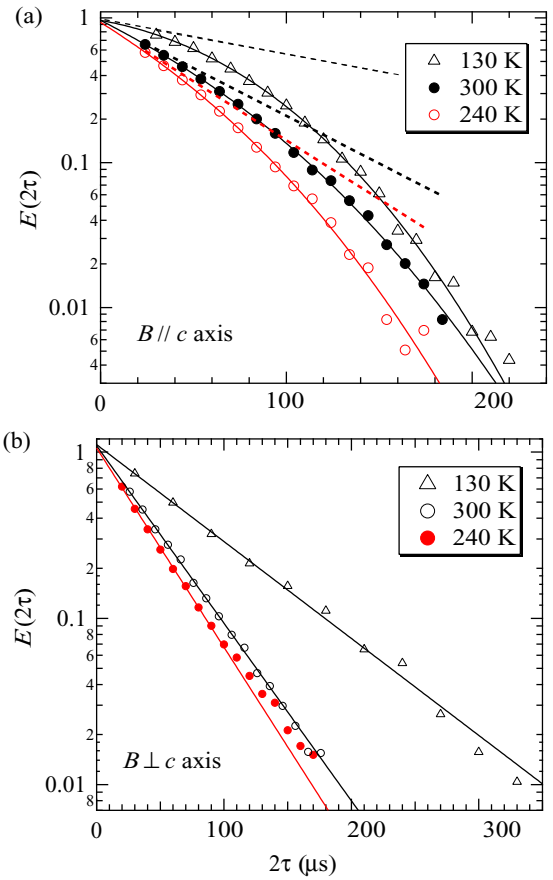

FIG. 2. (a) Transverse relaxation curves $E(2\tau)$ of the ^{63}Cu nuclear spin echo for the optimally doped Hg1212 ($T_c = 127$ K) at 130, 240, and 300 K ($B \parallel c$ axis). Solid curves are the least-squares fitting results using Eq. (1). As visual guides, dashed lines indicate single exponential functions with T_{2L} isolated from Eq. (1). (b) Transverse relaxation curves $E(2\tau)$ of the ^{63}Cu nuclear spin echo at 130, 240, and 300 K ($B \perp c$ axis). Solid lines are the least-squares fitting results using a single exponential function.

for the $B \parallel c$ axis. No H_1 dependence of the spin-echo decay was also observed for the $B \perp c$ axis.

Figures 1(b) and 1(c) show the ^{63}Cu nuclear spin-echo transverse relaxation curves $E(2\tau)$ of the central transition lines for the $B \parallel c$ axis [Fig. 1(b)] and $B \perp c$ axis [Fig. 1(c)]. Solid curves are the least-squares fitting results using Eq. (1). The Gaussian component for the $B \perp c$ axis was negligible, which indicates a weak-coupling constant of $I_{\pm}I_{\mp}$ (the in-plane components of the nuclear spin I) and no contribution from the nonsecular mutual spin-flip terms [25,26].

Figure 2 shows the temperature dependence of the ^{63}Cu nuclear spin-echo transverse relaxation curve $E(2\tau)$ for the $B \parallel c$ axis [Fig. 2(a)] and for the $B \perp c$ axis [Fig. 2(b)]. In Fig. 2(a), solid curves are the least-squares fitting results using Eq. (1). For the $B \parallel c$ axis, the initial decay of $E(2\tau)$ at 240 K is faster than that at 130 and 300 K, which is shown by the dashed lines. In Fig. 2(b), solid lines are the least-squares fitting results using a single exponential function. For the $B \perp c$ axis, the exponential decay of $E(2\tau)$ at 240 K is faster than that at 130 and 300 K.

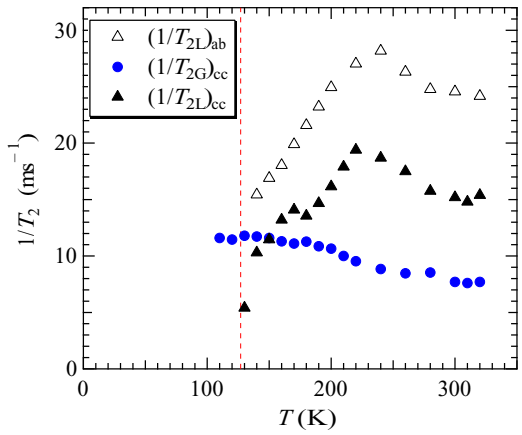

FIG. 3. Transverse relaxation rates $(1/T_{2L})_{cc}$, $(1/T_{2G})_{cc}$, and $(1/T_{2L})_{ab}$ of the ^{63}Cu nuclear spin echo for the optimally doped Hg1212 ($T_c = 127$ K). The dashed line indicates $T_c = 127$ K.

III. TRANSVERSE RELAXATION RATES

Figure 3 shows ^{63}Cu nuclear spin-echo transverse relaxation rates $(1/T_{2L})_{cc}$, $(1/T_{2G})_{cc}$, and $(1/T_{2L})_{ab}$ for the optimally doped Hg1212 ($T_c = 127$ K). The subscript index α $(= a,b,c)$ stands for the orientation of an external magnetic field B along the α axis. $(1/T_{2L})_{ab}$ is the relaxation rate for the $B \perp c$ axis. Both $(1/T_{2L})_{cc}$ and $(1/T_{2L})_{ab}$ show an enhancement at 220–240 K, which we call the T_2 anomaly.

For the central transition line ($I_z = \frac{1}{2} \leftrightarrow -\frac{1}{2}$) of a nuclear spin $I = \frac{3}{2}$, the transverse relaxation rate $(1/T_{2L})_{\gamma\gamma}$ is expressed as

$$\left(\frac{1}{T_{2L}}\right)_{\gamma\gamma} = \frac{7}{2}[J_{\alpha\alpha}(\nu_n) + J_{\beta\beta}(\nu_n)] + J_{\gamma\gamma}(0), \tag{2}$$

where $J_{\alpha\alpha}(\nu_n)$ (α,β,γ is the cyclic permutation of a,b,c) is the α component of the local field fluctuations at the NMR frequency ν_n [9,10,17,27,28]. $J_{\alpha\alpha}(\nu_n)$ is expressed by the hyperfine coupling constants $A_{\alpha\alpha}$ and the electron spin-spin correlation function $S_{\alpha\alpha}(\boldsymbol{q},\nu)$,

$$J_{\alpha\alpha}(\nu_n) = \sum_{\boldsymbol{q}} A_{\alpha\alpha}(\boldsymbol{q})^2 S_{\alpha\alpha}(\boldsymbol{q},\nu_n), \tag{3}$$

where $S_{\alpha\alpha}(\boldsymbol{q},\nu)$ is related to the dynamical spin susceptibility $\chi''(\boldsymbol{q},\omega)$ through the fluctuation-dissipation theorem [9,10,17]. The nuclear spin-lattice relaxation rate $(1/T_1)_{\gamma\gamma}$ is expressed as

$$\left(\frac{1}{T_1}\right)_{\gamma\gamma} = J_{\alpha\alpha}(\nu_n) + J_{\beta\beta}(\nu_n). \tag{4}$$

A conventional fluctuation spectrum is independent of the frequency in the NMR frequency region and then $J_{\gamma\gamma}(0) = J_{\gamma\gamma}(\nu_n)$ should hold. If $J_{\gamma\gamma}(0) = J_{\gamma\gamma}(\nu_n)$, $1/T_{2L}$ should agree with the Redfield relaxation rate $1/T_{2R}$ in Refs. [7,27,29] from the anisotropic T_1's. We estimate $1/T_{2R}$ from

$$\left(\frac{1}{T_{2R}}\right)_{cc} = 3\left(\frac{1}{T_1}\right)_{cc} + \left(\frac{1}{T_1}\right)_{ab}, \tag{5}$$

$$\left(\frac{1}{T_{2R}}\right)_{ab} = \frac{7}{2}\left(\frac{1}{T_1}\right)_{ab} + \frac{1}{2}\left(\frac{1}{T_1}\right)_{cc}, \tag{6}$$

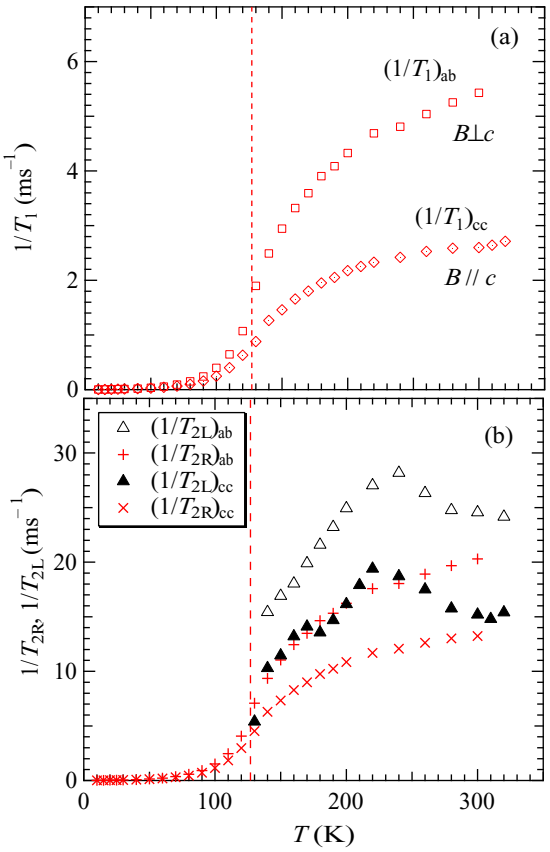

FIG. 4. (a) ^{63}Cu nuclear spin-lattice relaxation rates $(1/T_1)_{cc}$ and $(1/T_1)_{ab}$ for the optimally doped Hg1212 ($T_c = 127$ K). (b) ^{63}Cu nuclear spin-echo transverse relaxation rates $(1/T_{2L})_{cc}$ and $(1/T_{2L})_{ab}$. $(1/T_{2R})_{cc}$ and $(1/T_{2R})_{cc}$ were estimated using the Redfield theory [9] from the anisotropic T_1's in (a). The dashed line indicates $T_c = 127$ K.

according to uniaxially symmetric fluctuations ($J_{aa} = J_{bb}$ is then denoted by J_{ab}) [7,27,29–32]. $(1/T_{2R})_{ab}$ is the relaxation rate for the $B \perp c$ axis.

Figure 4(a) shows ^{63}Cu nuclear spin-lattice relaxation rates $(1/T_1)_{cc,ab}$ for the optimally doped Hg1212. No frequency dependence was observed at 85–115 MHz. Figure 4(b) shows ^{63}Cu nuclear spin-echo transverse relaxation rates $(1/T_{2L})_{cc,ab}$ and the Redfield relaxation rates $(1/T_{2R})_{cc,ab}$ estimated from the anisotropic T_1 using Eqs. (5) and (6). In Fig. 4(b), the enhancement in $(1/T_{2L})_{\gamma\gamma}$ at 220–240 K is not reproduced from $(1/T_{2R})_{\gamma\gamma}$.

Let us define $\Delta J_{\gamma\gamma}$ as

$$\Delta J_{\gamma\gamma} = \left(\frac{1}{T_{2L}}\right)_{\gamma\gamma} - \left(\frac{1}{T_{2R}}\right)_{\gamma\gamma}, \tag{7}$$

which can be a criterion to test whether the characteristic fluctuation frequency is higher or lower than the NMR frequency. Figure 5 shows the temperature dependences of ΔJ_{cc} and ΔJ_{ab} for the optimally doped Hg1212. For the $B \parallel c$ axis, ΔJ_{cc} is equal to $J_{cc}(0) - J_{cc}(\nu_n)$. Figure 5 indicates $\Delta J_{cc} > 0$ and $J_{cc}(0)$ strongly enhanced at 220–240 K. The characteristic frequency should be lower than the NMR frequency. Different ultraslow fluctuations develop in the pseudogap state.

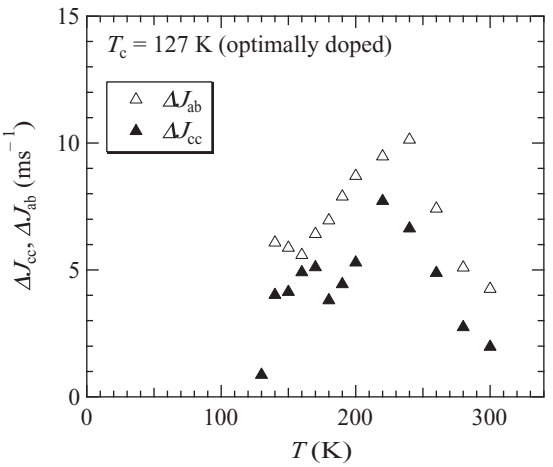

FIG. 5. ΔJ_{cc} and ΔJ_{ab} against temperature for the optimally doped Hg1212.

Isotope measurements could be helpful to specify whether the relaxation mechanism is magnetic or electric, because the isotope ^{65}Cu has a smaller quadrupole moment than ^{63}Cu while the nuclear gyromagnetic ratio is larger. However, since our T_{2L} values of ^{65}Cu were not conclusive due to the poor signal intensity, the effects of the charge fluctuations are unclear.

Figure 6(a) shows $(1/T_{2L})_{cc}$ against temperature for Hg1212 from underdoped ($T_c = 103$ K) to overdoped ($T_c = 93$ K). Figure 6(b) shows the doping dependence of $(1/T_1)_{cc}$ against temperature. The doping dependence of $(1/T_{2L})_{cc}$ is different from that of $(1/T_1)_{cc}$. The peak temperature of $(1/T_{2L})_{cc}$ is nearly independent of the doping level, but the enhancement in $(1/T_{2L})_{cc}$ is suppressed by overdoping. The peak temperature of $(1/T_{2L})_{cc}$ is similar to but deviates from the spin-pseudogap temperature defined by the maximum of the ^{63}Cu $1/T_1T$ [14].

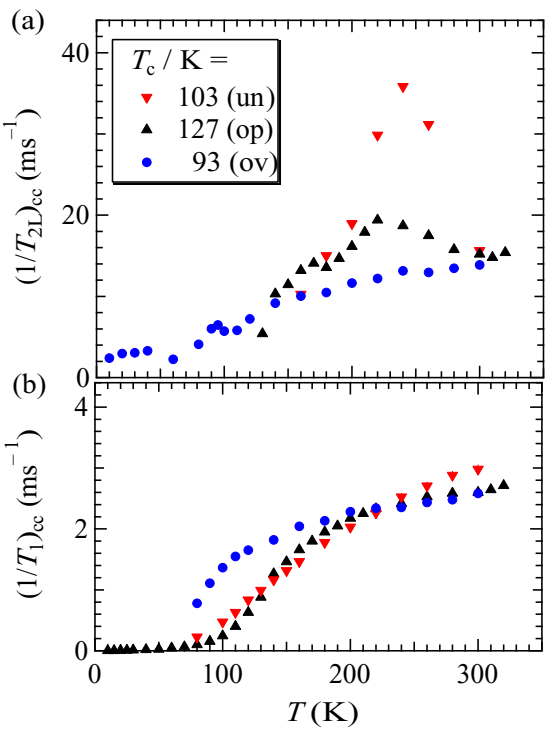

FIG. 6. (a) Doping dependence of $(1/T_{2L})_{cc}$ against temperature for Hg1212 from underdoped ($T_c = 103$ K) to overdoped ($T_c = 93$ K). (b) Doping dependence of $(1/T_1)_{cc}$ against temperature for Hg1212 from underdoped ($T_c = 103$ K) to overdoped ($T_c = 93$ K).

IV. DISCUSSIONS

As the carrier concentration increases, the spin-pseudogap temperature of ^{63}Cu $1/T_1T$ decreases and the peak value increases [14], being in contrast to $(1/T_{2L})_{cc}$ in Fig. 6(a). Thus, the local field fluctuations causing ^{63}Cu $(1/T_{2L})_{cc}$ at 220–240 K must be different from those causing ^{63}Cu $1/T_1T$.

For Hg1212, we infer an ultraslow fluctuation spectrum of $\chi''_L(q,\omega)/\omega = \chi_L(q\xi)\Gamma_L(q\xi)/[\omega^2 + \Gamma_L^2(q\xi)]$ $(\omega = 2\pi\nu)$ with a characteristic energy scale $\Gamma_L(q\xi) \ll 2\pi\nu_n$ (an ultraslow condition) and a correlation length ξ [33], in addition to the antiferromagnetic spin fluctuation model [34–36]. Then, we obtain $1/T_1 \ll \chi_L(0)/\Gamma_L(0) \sim 1/T_{2L}$, which shows a peak at 220–240 K for Hg1212.

The emergence of ultraslow fluctuations has been reported near the charge-spin stripe ordering temperature and the phase boundary in La-based 214 systems (LSCO) [18–20,33]. The wipeout effect on NMR/NQR signals is also characteristic of LSCO [18–20]. Hg1212, however, shows no wipeout effect on the Cu NMR spectrum nor any glassy behavior in the pseudogap state. The T_2 anomaly of Hg1212 is a homogeneous phenomena.

In $La_{1.6-x}Nd_{0.40}Sr_xCuO_4$, the transverse relaxation rate $1/^{139}T_2$ of the ^{139}La nuclear spin shows a peak at about 20 K above T_c and below the charge ordering temperature $T_{charge} \sim 70$ K [18], and $1/^{63}T_{2L}$ of the ^{63}Cu nuclear spin shows a peak at about 15 or 50 K [19]. In $La_{1.68}Eu_{0.20}Sr_{0.12}CuO_4$, the ^{139}La nuclear spin-lattice relaxation rate $1/^{139}T_1$ also shows a peak above T_c and below T_{charge}, while ^{63}Cu $1/^{63}T_1$ shows a weak upturn on cooling below T_{charge} [19,20]. The ^{139}La nuclear spin plays a role in detecting lower frequency fluctuations than the ^{63}Cu nuclear spin. The difference in the relaxation rates between ^{139}La and ^{63}Cu for (Nd, Eu)-doped LSCO is parallel to that between ^{63}Cu $1/^{63}T_{2L}$ and $1/^{63}T_1$ for Hg1212 in Fig. 6. For the time being, it is unlikely that Hg1212 is in a charge ordering state at 220–240 K, because the high electrical conductivity shows a metallic behavior [37,38]. The ultraslow fluctuation spectrum $\chi''_L(q,\omega)/\omega$ of Hg1212 may be a part of the charge-spin stripe fluctuation spectrum but should describe a purely fluctuating stripe.

Recent experimental efforts have revealed several hidden orders in the pseudogap states: quadrupolar fluctuations below 200 K in $YBa_2Cu_4O_8$ [39], the onset T_{CDW} of a short-ranged charge density wave [5,40], the development of an intra-unit-cell local magnetic order [41], and the onset of finite Kerr rotations [42]. The T_2 anomaly of Hg1212 may correspond to one of these short-ranged orders, because $(1/T_{2L})_{cc}$ shows a peak but not divergence. These findings suggest that the pseudogap state is not a simple spin-singlet state.

V. CONCLUSIONS

In conclusion, we found enhanced zero frequency local field fluctuations at 220–240 K for Hg1212 in the pseudogap states through ^{63}Cu nuclear spin-echo transverse relaxation, which suggests the emergence of ultraslow fluctuations. Interesting ultraslow fluctuations without any glassy behavior are hidden in the pseudogap states.

[1] I. Iguchi, T. Yamaguchi, and A. Sugimoto, Nature (London) **412**, 420 (2001).

[2] Y. Wang, L. Li, M. J. Naughton, G. D. Gu, S. Uchida, and N. P. Ong, Phys. Rev. Lett. **95**, 247002 (2005).

[3] L. Li, Y. Wang, S. Komiya, S. Ono, Y. Ando, G. D. Gu, and N. P. Ong, Phys. Rev. B **81**, 054510 (2010).

[4] T. Wu, H. Mayaffre, S. Krämer, M. Horvatić, C. Berthier, W. N. Hardy, R. Liang, D. A. Bonn, and M.-H. Julien, Nature (London) **477**, 191 (2011).

[5] M. Hücker, N. B. Christensen, A. T. Holmes, E. Blackburn, E. M. Forgan, R. Liang, D. A. Bonn, W. N. Hardy, O. Gutowski, M. v. Zimmermann, S. M. Hayden, and J. Chang, Phys. Rev. B **90**, 054514 (2014).

[6] R. Comin, R. Sutarto, E. H. da Silva Neto, L. Chauviere, R. Liang, W. N. Hardy, D. A. Bonn, F. He, G. A. Sawatzky, and A. Damascelli, Science **347**, 1335 (2015).

[7] C. H. Pennington, D. J. Durand, C. P. Slichter, J. P. Rice, E. D. Bukowski, and D. M. Ginsberg, Phys. Rev. B **39**, 274 (1989).

[8] C. H. Pennington and C. P. Slichter, Phys. Rev. Lett. **66**, 381 (1991).

[9] C. P. Slichter, *Principles of Magnetic Resonance*, 3rd ed. (Springer, New York, 1990).

[10] T. Moriya, Prog. Theor. Phys. **16**, 641 (1956).

[11] T. Moriya, Prog. Theor. Phys. **28**, 371 (1962).

[12] Y. Itoh, H. Yasuoka, Y. Fujiwara, Y. Ueda, T. Machi, I. Tomeno, K. Tai, N. Koshizuka, and S. Tanaka, J. Phys. Soc. Jpn. **61**, 1287 (1992).

[13] Y. Itoh, J. Phys. Soc. Jpn. **63**, 3522 (1994); **64**, 684 (1995).

[14] Y. Itoh, A. Tokiwa-Yamamoto, T. Machi, and K. Tanabe, J. Phys. Soc. Jpn. **67**, 2212 (1998).

[15] T. Imai, C. P. Slichter, K. Yoshimura, M. Katoh, and K. Kosuge, Phys. Rev. Lett. **71**, 1254 (1993).

[16] M. Takigawa, O. A. Starykh, A. W. Sandvik, and R. R. P. Singh, Phys. Rev. B **56**, 13681 (1997).

[17] V. Jaccarino, in *Theory of Magnetism in Transition Metals*, Proceedings of the International School of Physics "Enrico Fermi," Course XXXVII, Varenna, 1966, edited by W. Marshall (Academic Press, New York, 1967), p. 335.

[18] G. B. Teitel'baum, I. M. Abu-Shiekah, O. Bakharev, H. B. Brom, and J. Zaanen, Phys. Rev. B **63**, 020507(R) (2000).

[19] P. M. Singer, A. W. Hunt, A. F. Cederström, and T. Imai, Phys. Rev. B **60**, 15345 (1999).

[20] A. W. Hunt, P. M. Singer, A. F. Cederström, and T. Imai, Phys. Rev. B **64**, 134525 (2001).

[21] S. N. Putilin, E. V. Antipov, and M. Marezio, Physica C **212**, 266 (1993).

[22] A. Fukuoka, A. Tokiwa-Yamamoto, M. Itoh, R. Usami, S. Adachi, and K. Tanabe, Phys. Rev. B **55**, 6612 (1997).

[23] N. J. Curro, T. Imai, C. P. Slichter, and B. Dabrowski, Phys. Rev. B **56**, 877 (1997).

[24] N. J. Curro and C. P. Slichter, J. Magn. Reson. **130**, 186 (1998).

[25] T. Imai, C. P. Slichter, A. P. Paulikas, and B. Veal, Phys. Rev. B **47**, 9158(R) (1993).

[26] Y. Itoh, Ph.D. thesis, University of Tokyo, 1994.

[27] C. H. Pennington, Ph.D. thesis, University of Illinois, 1993.

[28] To be more precise, a local field fluctuation in $1/T_{2R}$ of the central transition line is also a function of the Larmor frequencies of $I_z = \pm\frac{3}{2} \leftrightarrow \pm\frac{1}{2}$.

[29] T. Auler, P. Butaud, and J. A. Gillet, J. Phys.: Condens. Matter **8**, 6425 (1996).

[30] R. E. Walstedt, *The NMR Probe of High-T_c Materials* (Springer, New York, 2008).

[31] R. E. Walstedt, Phys. Rev. Lett. **19**, 146 (1967); **19**, 816 (1967).

[32] A. Narath, Phys. Rev. B **13**, 3724 (1976).

[33] Y. Itoh, T. Machi, N. Koshizuka, M. Murakami, H. Yamagata, and M. Matsumura, Phys. Rev. B **69**, 184503 (2004).

[34] N. Bulut, D. W. Hone, D. J. Scalapino, and N. E. Bickers, Phys. Rev. B **41**, 1797 (1990).

[35] T. Moriya, Y. Takahashi, and Y. Ueda, J. Phys. Soc. Jpn. **59**, 2905 (1990).

[36] A. J. Millis, H. Monien, and D. Pines, Phys. Rev. B **42**, 167 (1990).

[37] A. Ogawa, T. Sugano, H. Wakana, A. Kamitani, S. Adachi, Y. Tarutani, and K. Tanabe, Jpn. J. Appl. Phys. **43**, L40 (2004).

[38] A. Ogawa, T. Sugano, H. Wakana, A. Kamitani, S. Adachi, Y. Tarutani, and K. Tanabe, Jpn. J. Appl. Phys. **97**, 013903 (2005).

[39] A. Suter, M. Mali, J. Roos, and D. Brinkmann, Phys. Rev. Lett. **84**, 4938 (2000).

[40] T. Wu, H. Mayaffre, S. Krämer, M. Horvatić, C. Berthier, W. N. Hardy, R. Liang, D. A. Bonn, and M.-H. Julien, Nat. Commun. **6**, 6438 (2015).

[41] Y. Sidis and P. Bourges, J. Phys.: Conf. Ser. **449**, 012012 (2013).

[42] J. Xia, E. Schemm, G. Deutscher, S. A. Kivelson, D. A. Bonn, W. N. Hardy, R. Liang, W. Siemons, G. Koster, M. M. Fejer, and A. Kapitulnik, Phys. Rev. Lett. **100**, 127002 (2008).